SAN097-0110C

# THE EFFECT OF STRESS ON THE NANOMECHANICAL PROPERTIES OF Au SURFACES

CONF-961202--23

SAND--97-0110C

J. E. Houston
Sandia National Laboratories
Albuquerque, NM 87185-1413

## ABSTRACT

Stress in thin films plays a critical role in many technologically important areas. The role is a beneficial one in strained layer superlattices where semiconductor electrical and optical properties can be tailored with film stress. On the negative side, residual stress in thin-film interconnects in microelectronics can lead to cracking and delamination. In spite of their importance, however, surface and thin-film stresses are difficult to measure and control, especially on a local level. In recent studies, we used the Interfacial Force Microscope (IFM) in a nanoindenter mode to survey the nanomechanical properties of Au films grown on various substrates. Quantitative tabulations of the indentation modulus and the maximum shear stress at the plastic threshold showed consistent values over individual samples but a wide variation from substrate to substrate. These values were compared with film properties such as surface roughness, average grain size and interfacial adhesion and no correlation was found. However, in a subsequent analysis of the results, we found consistencies which support the integrity of the data and point to the fact that the results are sensitive to some property of the various film/substrate combinations. In recent measurements on two of the original substrate materials we found a direct correlation between the nanomechanical values and the residual stress in the films, as measured globally by a wafer warping technique. In the present paper, we review these earlier results and show recent measurements dealing with stresses externally applied to the films which supports our earlier conclusion concerning the role of stress on our measurements. In addition, we present very recent results concerning morphological effects on nanomechanical properties which add additional support to the suggestion that near-threshold indentation holds promise of being able to measure stress on a very local level.

## INTRODUCTION

As the structure of advanced materials become ever smaller (the so-called nanophase materials) and the sizes of electromechanical devices shrink (into the realm of nanofabrication), it becomes increasingly important to be able to determine material properties on the nanometer scale. In recent work, we have explored the use of the Interfacial Force Microscope (IFM) in studies of the nanomechanical properties of surfaces [1-3]. The IFM is a scanning force microscope similar to the atomic force microscope but is distinguished by its use of a stable, self-balancing force sensor. Not only does this sensor eliminate the ɔsnap to contact so prevalent in adhesion, scanning probe and indenter studies; but it is also a zero-compliance sensor, i.e., an applied force produces no sensor displacement and no sensor-stored energy. This work involved a parabolic W tip indenting Au thin-film surfaces which had been passivated by a monolayer of



DISTRIBUTION OF THIS DOCUMENT IS UNLIMITED

MASTER

DISCLAIMER

**Portions of this document may be illegible in electronic image products. Images are produced from the best available original document.**

# DISCLAIMER

This report was prepared as an account of work sponsored by an agency of the United States Government. Neither the United States Government nor any agency thereof, nor any of their employees, make any warranty, express or implied, or assumes any legal liability or responsibility for the accuracy, completeness, or usefulness of any information, apparatus, product, or process disclosed, or represents that its use would not infringe privately owned rights. Reference herein to any specific commercial product, process, or service by trade name, trademark, manufacturer, or otherwise does not necessarily constitute or imply its endorsement, recommendation, or favoring by the United States Government or any agency thereof. The views and opinions of authors expressed herein do not necessarily state or reflect those of the United States Government or any agency thereof.

alkanethiol self-assembling molecules (SAM). Under these conditions, the normally strong W-Au interfacial interaction is eliminated and classic Hertzian contact mechanics is observed.

In order to investigate the efficacy of the IFM for nanomechanical studies, we surveyed a series of Au films grown under various conditions on various substrates [4]. Values were tabulated for the elastic modulus and the maximum shear stress at the plastic threshold by averaging the measurements many times on each film/substrate combination. The results were very consistent for each of the individual samples but varied widely between the various substrates. The source of the variation was not known and it was speculated to be the result of film properties such as grain size, surface roughness or film adhesion. However, no direct correlation was found between the results and these various parameters. Subsequent work indicated that the unusual behavior correlated with the residual stress in the films caused by the interfacial mismatch between the film and substrate. In the present paper, we review these earlier results and show more recent measurements dealing with stresses externally applied to the films which support our earlier conclusion concerning the role of stress. In addition, we show our most recent results concerning morphological effects on nanomechanical properties, which add additional support to the suggestion that near-threshold indentation holds promise of being able to measure film stress on a very local level.

In order to measure nanomechanical properties we collect data on the force of interaction between a W probe and a Au surface as a function of sample displacement (force profiles). To illustrate the nature of the data, we show in Fig. 1 a typical force profile for a 250 nm radius W probe indenting a 200 nm Au film deposited on a glass substrate. These data were obtained by ramping the probe at a constant rate (2.0 nm/sec) into contact with the Au surface. The direction of the probe motion was reversed after a certain level of repulsive force was attained, and the probe was withdrawn from contact at the same rate. Data like that in Fig. 1 were analyzed by standard contact-mechanics techniques [5]. The initial rise of the force with displacement is elastic and follows the Hertzian relationship (shown as the solid line in Fig. 1), while the deviation from this behavior signals the onset of plasticity. In the plastic region, several rapid drops in force result from sudden material relaxation (nano-quake events). These are only seen in this form with a zero-compliance sensor.

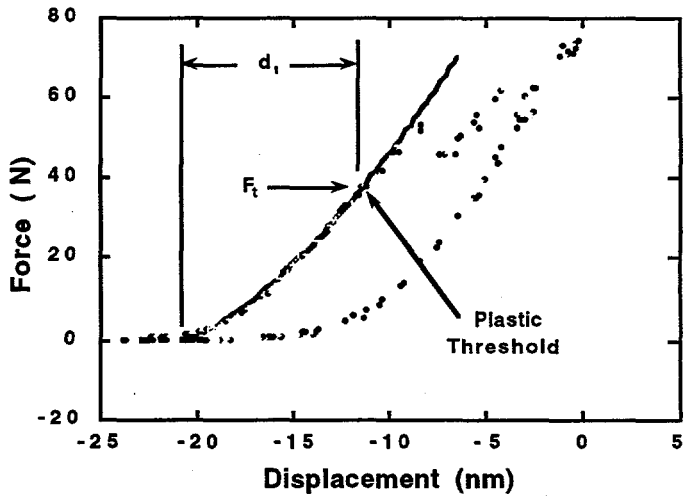


Figure 1. A typical loading curve for a 200 nm Au film on a glass substrate. The solid line illustrates the fit of the Hertzian relationship to the data, which permits an evaluation of the quantities $F_t$ and $d_t$.

The importance of the passivating thiol molecular monolayer cannot be overemphasized. To illustrate the point, we show in Fig. 2 the results of a clean W tip contacting a clean Au(111) surface (data taken in a newly developed UHV/IFM [6]). Under these circumstances, the surfaces suddenly ɜjump-to-contact and eventually form a very strong adhesive bond. This bond is so strong, in fact, that it creates the defects which give rise to plastic deformation at contact. The 120 Å extent of the interaction to the point of zero applied force results from the

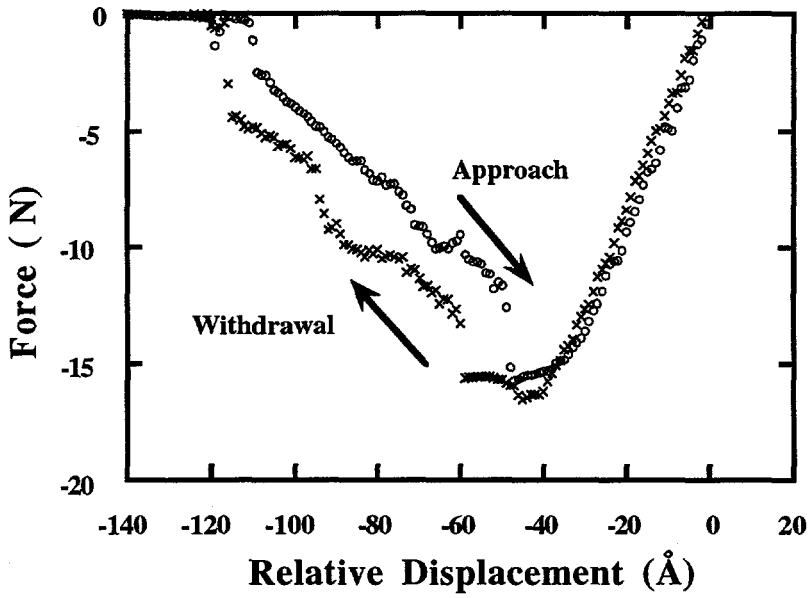


Figure 2. A typical force profile for a clean surfaces of a 2000 Å W tip and a Au(111) sample taken under UHV conditions.

plastic flow of the Au surface under only the force of adhesive attraction. Achieving the plastic threshold deformation in the passivated case of Fig. 1 requires an externally applied repulsive force of about 40 N, while in the non-passivated case, plasticity occurs upon initial contact. The thiol passivation completely eliminates the adhesive interaction and permits a classic elastic contact-mechanics analysis of the nanomechanical properties of the sample.

## RESULTS

In the original thin-film survey, the films consisted of 200 nm thick Au deposited on cleaned surface of glass, mica and Si(001) with both 10 nm adhesion layers of Ti and Cr [4]. The glass and mica depositions were done at 300 C followed by a 3 hr anneal at 275 C while the Au/Si depositions were done at room temperature. The films were then cleaned and a SAM (n-octadecanethiol) deposited. All measurements were made with the same sensor and 250 nm radius W tip and the probe was immersed in a drop of hexadecane to suppress the attractive van der Waal s interaction.

The initial portion of the loading curve after contact (see Fig. 1) can be characterized by the Hertzian relation,

$$F = \frac{4}{3}\sqrt{R}\cdot E\cdot d^{\frac{3}{2}}, \qquad (1)$$

where F is the applied probe force, R is the radius of the tip, E is the elastic modulus and d is the deformation. From the fit of this expression to the data (shown as the solid curve in Fig. 1) and a knowledge of the tip radius, one can calculate the modulus value. The force and deformation at the point where the loading curve deviates from the Hertzian behavior signals the onset of plasticity. The maximum shear stress at this point can be calculated from the expression [5],

$$S_m = 0.47\cdot\frac{F_t}{\pi\cdot R d_t}, \qquad (2)$$

where $S_m$ is the maximum shear stress and $F_t$ and $d_t$ are the probe force and deformation values at the plastic threshold (see Fig. 1).

Table I. Summary of the findings in the study of nanomechanical properties of 200 nm Au films grown on various substrates and for single-crystal Au(111) [4].

| Sample | Elastic Modulus E (Gpa) | Max. Shea $S_m$ (Gpa) | Grain Diameter (nm) | Roughness (nm) | Substrate Adhesion |
|---|---|---|---|---|---|
| Au/Mica | 36 ± 5 | 1.7 ± 0.2 | 250 | 5.4 | Very Weak |
| Au/Ti/Si | 48 ± 5 | 2.1 ± 0.3 | 60 | 1.8 | Strong |
| Au/Glass | 75 ± 15 | 2.7 ± 0.5 | 500 | 4.1 | Weak |
| Au/Cr/Si | 110 ± 19 | 4.5 ± 0.4 | 150 | 2.4 | Very Strong |
| Au(111) | 70 ± 6 | 2.9 ± 0.1 | | | |

Table I shows the results of our survey tabulated in ascending order of the modulus values. The error figures represent the statistical variation over 15-20 individual loading curves for each film/substrate combination and the value for single-crystal Au(111) has been included for comparison. Also shown are the values for the average grain sizes and the mean surface roughness of the surface for the various film/substrate combinations, as well as a column representing recent qualitative measurements of the film/substrate adhesion obtained from simple adhesive-tape stripping and stylus scratch tests.

As can be seen from Table I, the E and $S_m$ values vary by almost a factor of three when, in fact, one would expect them to remain constant. In addition, it is clear that there is no correlation of this variation with any of the other film parameters listed. However, a consistency in the data, which was not noted in the earlier publication [4], concerns the fact that the E and $S_m$ values vary in the same way as the substrates are changed. In fact, the ratio $S_m/E$ is very close to being constant at 4%. The ratio of $S_m/E$ is a common figure of merit in material science and, in fact, can

be crudely calculated from the Frenkel approximation to be ~5.5% [7]. Furthermore, if Eq. (1) is substituted into Eq. (2), we can show that a constant $S_m/E$ ratio implies that the deformation to the plastic threshold $d_t$ should also be a constant. Table II tabulates the narrow range of variation of these two constants for the various film/substrate combinations.

Table II. Values for the ratio $S_m/E$ and the measured values of $d_t$ for the various film/substrate combinations.

| Sample | $S_m/E$ (%) | $d_t$ (nm) |
|---|---|---|
| Au/Mica | 4.7 | $13 \pm 1$ |
| Au/Ti/Si | 4.4 | $15 \pm 2$ |
| Au/Glass | 3.6 | $9 \pm 1$ |
| Au/Cr/Si | 4.1 | $13 \pm 2$ |

The remarkable consistency in the two parameters shown in Table II, in spite of the wide variation in film properties for the various substrates, strongly suggests that the wide range in measured E and $S_m$ values has its origin in some extrinsic film property. A possible clue to this property can be found in the recent work with the nanoindenter on Al samples under lateral stress. Pharr and coworkers discussed earlier indentation work on films under stress and shows data for Al samples under applied lateral stress using a four-fold diamond Berkovich probe well beyond the initial plastic threshold. The results show a dependence of the measured modulus and hardness values on the applied lateral stress in the sample such that the ratio of the values remained essentially constant [8].

While this is an intriguing possible explanation for our earlier results, there are several features which are different. First, the effect was only found to be at the 10% level. Second, Pharr, et al. concluded that the variation in values results from a stress-induced ɔpileup of material at the periphery of the contact. Compressive stress causes additional pileup while tensile stress reduces the effect. The pileup changes the contact area and affects the apparent mechanical properties. When the loading curves were corrected for the measured contact areas, the effect disappeared. Still, varying residual stresses in thin films are known to exist and the effect on near-threshold indentation results bears investigation.

As a preliminary look at the effect of residual film stress on near-threshold indentation results, we measured the stresses in identically prepared films for two of our four film/substrate combinations, i.e., 200 nm Au films deposited at room temperature on Si(001) substrates with 10 nm Cr and Ti adhesion layers. The stresses were obtained using a wafer-curvature technique [9] which measures film stress by determining the change in wafer warping before and after the deposition of the film. This change, along with the elastic properties and thickness of the wafer material are used to calculate the value of film stress. The results of these measurements, along with the corresponding values from Table I, are tabulated in Table III.

The data in Table III represents the first of the parameters surveyed that show a positive correlation with our measured values. However, the nanomechanical and stress data were obtained on separately-prepared samples, which prompted an effort to accumulate addition data. More recent results, using an IFM-retrofitted Nanoscope III AFM instrument [10], involved

both sets of information taken on the same samples [11]. In addition, the Au depositions were done on sputter-cleaned Si(001) substrates and under more carefully controlled conditions.

Table III. The correlation between the E and $S_m$ values for two of the film/substrate combinations with the measured residual-film stress. The + sign indicates tensile stress.

| Sample | E (GPa) | $S_m$ (GPa) | Film Stress (MPa) |
|---|---|---|---|
| Au/Ti/Si(001) | $48 \pm 5$ | $2.1 \pm 0.3$ | -140 |
| Au/Cr/Si(001) | $110 \pm 19$ | $4.5 \pm 0.4$ | +325 |

These data are summarized in Table IV.

Table IV. A compilation of parameters for Au films grown on sputter-cleaned Si(001) substrates compared to that obtained from single-crystal Au(111).

| Film | Grain Diameter (nm) | Max. Peak-to-Valley (nm) | RMS Roughness (nm) | Total Film Thickness (nm) | Residual Stress (MpA) | Measured Elastic Modulus (GpA) |
|---|---|---|---|---|---|---|
| Au/Cr/Si | 40 6 | 10 1 | 1.2 0.04 | 115 15 | +100 40 | 84 2 |
| Au/Ti/Si | 45 8 | 13 1 | 1.3 0.06 | 105 8 | -40 20 | 65 3 |
| Au/Si | 35 8 | 28 2 | 3 2 | 101 9 | -35 25 | 55 10 |
| Au (111) | - | - | - | - | - | 70 |

## DISCUSSION

It is clear from the values tabulated in Tables I, III and IV that the only parameter showing a strong correlation with variations in E and $S_m$ is the residual-film stress. The values of both E and $S_m$ for Au/Ti/Si(001) and Au/Si are below those for Au(111) while those for Au/Cr/Si(001) are greater. The corresponding stress figures indicate a compressive stress for both Au/Ti/Si(001) and Au/Si while it is tensile for Au/Cr/Si(001). In fact, even the scaling of the magnitudes are close. Although these results are preliminary, it seems clear that the large variation in the near-threshold indentation measurements of E and $S_m$ for the various film/substrate combinations results from residual-film stress arising from the interfacial mismatch in structural properties for Au with the substrates. What is not clear from these results is the details of the mechanisms that are responsible for this

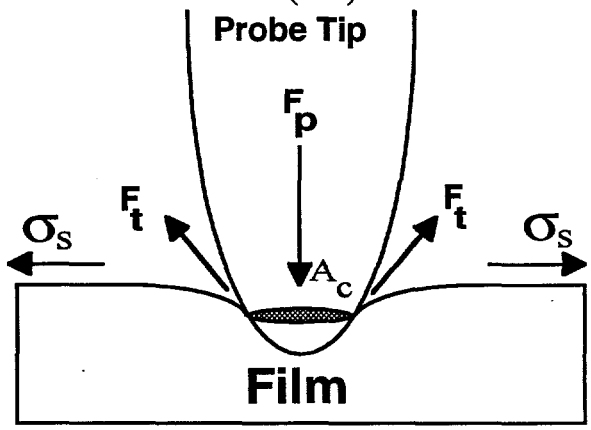


Figure 3. A simple model showing the effect of surface stress on the measured probe force.

correlation. One simple, intuitive model which suggest a relationship between lateral-film stress, at least surface stress, and the measured modulus is illustrated in Fig. 3. The surface stress $\sigma_s$ increases the Hertzian force by the normal component of the force $F_t$ tangent to the probe- tip contact surface. This force is equal to the surface stress times the contact area $A_c$. Solving for this component yields an equation for the probe force identical to Eq. (1) above except E is replaced by $E+\sigma_s$. Thus, surface stress would make the measured modulus appear larger as we see for tensile film stress. However, since E has a value of 70 Gpa, this equation severely underestimates the effect compared to our measurements, i.e., we measure about a 50% effect on the modulus with a film stress of less than one percent relative to E. Clearly, the problem is not as simple as implied by the model of Fig. 3. Elucidating these mechanisms will have to await more careful measurements with films whose lateral stress can be externally applied and accurately controlled over a broad range (in a manner such as that employed by Pharr and coworkers [8]), as well as calculations modeling experiments on similar systems.

In spite of the lack of a reasonable model to describe the stress sensitivity, our most recent results continue to be provocative. In these experiments indentation of the kind just discussed was done in the neighborhood of morphological features on a carefully prepared single-crystal Au(111) surface [12]. The sample was prepared in a UHV environment by repeated cycles of inert-ion sputtering and 800 C annealing. The process was repeated until good scanning tunneling microscopy (STM) images of the reconstructed Au surface were obtained. The sample was then removed from the vacuum system and immediately immersed in the thiol solution. This procedure stabilized the surface against contamination while it was being transferred to the IFM system for the nanoindentation experiments.

Figure 4 shows a repulsive force image of a 7500x7500 Å portion of the surface prepared as outlined above. This image was taken by raster-scanning the tip across the surface while holding the interfacial force at a small, constant value. The z position of the probe (the voltage supplied to the piezo xyz tube scanner) was then converted to a grey-scale i mage which is converted to a perspective view. The highly magnified z scale is represented by the 100 Å skirts on the image. Except for some particulate contamination, one of which is marked for future reference with a c, the surface appears very flat and is crossed by two single steps and one double step intersecting along the close-packed crystallographic axes. In order to investigate the effect of these subtle surface morphological defects, we now place our probe at various positions on the surface and perform nanoindentation experiments.

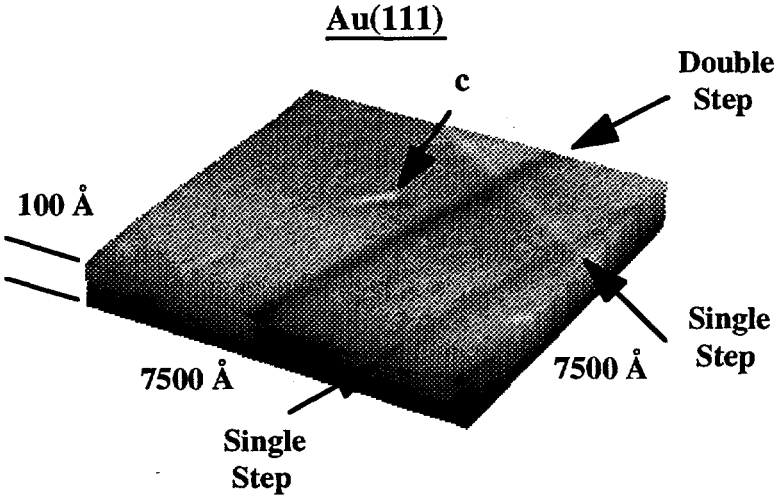


Figure 4. A repulsive-force image of a carefully prepared, thiol covered Au(111) surface. Single and double steps can be seen intersecting along crystallographic axes. As a reference, we have marked a contaminant particle with the symbol **c**.

In the first experiment, we place the probe on the flat terrace about 3000 Å to the left of the double step and particle **c** and obtain a force profile. The IFM-control software [13] is arranged to back the probe off of a slight repulsive-contact position by 20 Å followed by a linear approach at a speed of one Å/sec. The motion is reversed automatically when the software detects a plastic "event", i.e., where the repulsive force suddenly drops. The profile obtained in this manner is shown in Fig. 5. The probe tip used to obtain this profile was originally parabolic in shape with a 250 Å radius of curvature at the tip. However, the fact that the force is linearly increasing with approach displacement, in contrast to the normal Hertzian behavior of Fig. 1, indicates that this small tip has been flattened to approximate a cylindrical punch. Under these circumstances, the force vs. deformation will be linear and be given by the relation, $F=2REd$, where R is the radius of the punch, E the indentation modulus and d the deformation [5]. Matching the slopes in Fig. 5 to the expected modulus value indicates that the tip radius is about 250 Å. At about 12 μN, the repulsive force suddenly decreases as a result of a dramatic plastic relaxation of the Au surface. This is similar to a earth-quake event where the stress builds until suddenly there is some slippage which results in a abrupt stress relief. In this case, we have nucleated dislocations which give rise to the stress relief. To see what we have done to the surface, we show in Fig. 6 the image of the surface taken after the force profile of Fig. 5.

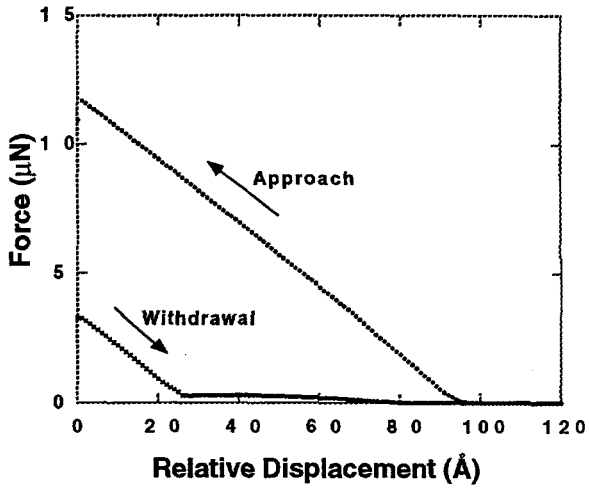


Figure 5. The force profile taken on the flat terrace away from any step boundaries.

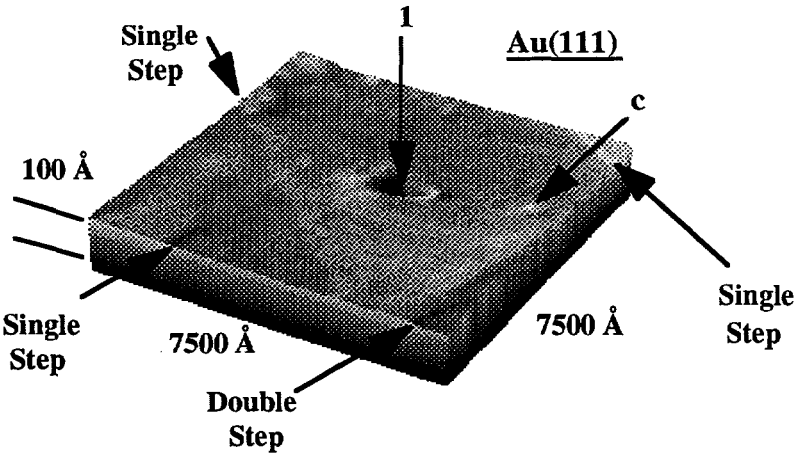


Figure 6. The dent resulting from the force profile of Fig. 5. The tip is ~3000 Å from the double step and more than 1000 Å form the closest of the two single steps.

The dent in Fig. 6 is more than 1000 Å from the nearest single step and ~3400 Å from the double step. The nominal diameter is ~750 Å and the depth is ~67 Å. The shear stress at the plastic threshold is particularly easy to calculate for a cylindrical indenter and is given by $S_t=F_t/\pi R^2$. This value turns out to be ~5.7 GPa from the maximum force value in Fig. 5. We can now directly compare the effect of surface morphology by collecting similar data at various probe positions.

Three more positions were probed, two of which are shown in Fig. 7. Dent number (2) is positioned ~650 Å from the double step on the "down" terrace while number (3) is located on the

"up" terrace ~1300Å from the double step. Finally in Fig. 8, we show dent (4) with the probe positioned to straddle the double step.

It first should be noted that the pile-up pattern for all the dents is triangular with sides aligned along directions parallel to the step edges, i.e., along close-packed directions of the (111) surface. Secondly, although not shown, the force profiles all appear very similar to that shown in Fig. 5 with essentially equal linear approach and withdrawal slopes and major plastic events. However, the force levels at the plastic thresholds vary markedly depending on position, indicating that the shear stress required to nucleate the plastic event depends on surface morphology. We summarize these result in Table V showing the calculated threshold shear stress for the various dents.

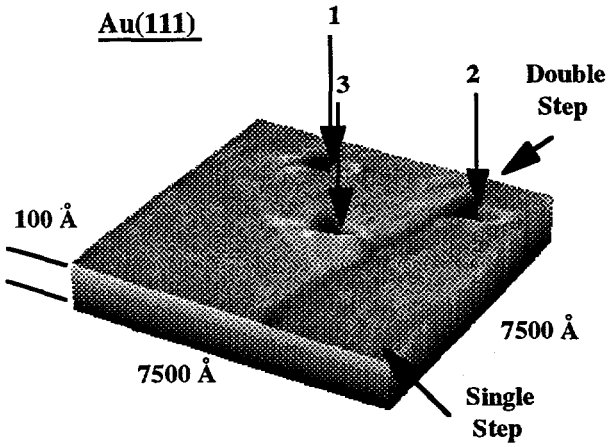


Figure 7. Additional dents with the tip located ~650 Å from the double step on the "down" terrace (2) and ~1300 Å from the double step on the "up" terrace (3). The depths are ~62 and ~53 Å, respectively.

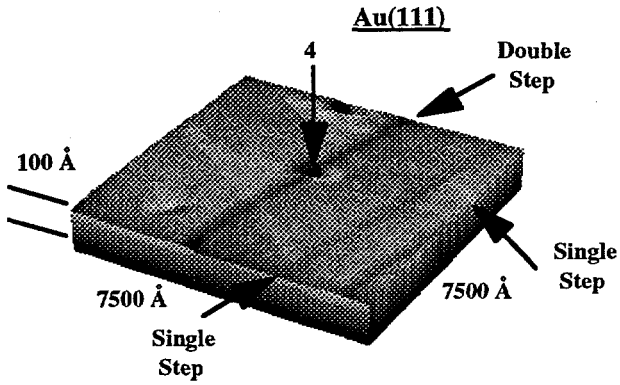


Figure 8. A dent placed astride the double step and positioned to the left of dent (3) along the double step in Fig. 7.

Table V. Summary of the result investigating the effect of steps on the nanomechanical properties of a single-crystal Au(111) surface.

| Distance from Step (Å) | Force at Plastic Threshold (μN) | Shear Stress at Plastic Threshold (GPa) | Depth of Dent (Å) |
|---|---|---|---|
| 3400 | 11.7 | 5.7 | 67 |
| 1300 | 11.1 | 5.4 | 62 |
| 570 | 9.8 | 4.8 | 53 |
| 0 | 7.3 | 3.6 | 29 |

Surface steps are reasonably subtle defects. However, because they set up an extended stress field they can have a profound effect on surface properties [14]. From the data of Table V we see that the presence of these morphological defects has a dramatic effect on the indentation behavior for measurements very near step edges causing the threshold shear stress to vary by more than 60%. At this point, the details of the mechanisms responsible for this variation are not clear, but they appear to be related to the earlier results involving thin-film stress effects.

## SUMMARY AND CONCLUSIONS

We have presented evidence that the near-threshold indentation experiment holds promise of being very sensitive to the presence of stress at the surface of the sample. In our earlier experiments we found consistent and reasonable values for the elastic modulus and the shear stress at the plastic threshold for individual thin-film samples but large variations in these values from substrate to substrate. The ratio of these two parameters, however, remained constant at about the theoretical value of 5.5%. We found no correlation between the shear stress and modulus values and any of the physical characteristics of the films (roughness, substrate adhesion, grain size, etc.). Subsequent measurements on similar films did show a correlation between the residual stress in the film and modulus/shear stress values. Subsequent work on a broader range of film/substrate combinations and on films with externally applied stress corroborated this correlation. Our most recent efforts have also showed a correlation between the plastic threshold shear stress and the distance of the indentation to steps on carefully prepared single-crystal Au(111) surface. Here again, the correlation appears to involve stress, since steps are known to create areas of stress which slowly diminishes away from the step edge [14]. At the present time, it is not clear just what the origin is for the sensitivity of near-threshold indentation to surface and films stress.

From these somewhat preliminary results, we have presented a strong argument that a sensitive link exists between near-threshold nanoindentation experiments and the stress condition of the surface being probed. This means that it may be possible to sensitively measure surface and thin-film stress at a very local level; measurements which are presently only possible at the local level on very thin samples by TEM or more globally by X-Ray diffraction and wafer-warping techniques. Such a capability will allow stress mapping and studies of its variation as a function of such important conditions as the presence of surface and interfacial adsorbates or adhesion-enhancing agents or to probe the effect of various environmental conditions on thin-film aging, to name only a very few. First, however, we must better establish the link and its physical origin. This will require experiments on films with carefully controlled and externally applied stress and reasonably sophisticated modeling of the indentation process.



## ACKNOWLEDGMENTS

The author wishes to express his gratitude to T. A. Michalske for program support and many stimulating discussions and to C. M. Matzke for sample preparation and performing the early residual stress measurements. This work was supported by the U. S. Department of Energy under Contract DE-AC04-94AL85000. Sandia is a multiprogram laboratory operated by Sandia Corporation, a Lockheed Martin Company, for the U. S. Department of Energy.

## REFERENCES


1. S. A. Joyce, R. C. Thomas, J. E. Houston, T. A. Michalske and R. M. Crooks, Phys. Rev. Lett. **68**, 2790 (1992).

2. R. C. Thomas,. J. E. Houston,. T. A. Michalske and R. M. Crooks, Science **259**, 1883 (1993).

3. P. Tangyunyong, R. C. Thomas, J. E. Houston, T. A. Michalske, R. M. Crooks and A. J. Howard, Phys. Rev. Lett. **71**, 3319 (1993).

4. P. Tangyunyong, R. C. Thomas, J. E. Houston, T. A. Michalske, R. M. Crooks and A. J. Howard, J. Adhes. Sci. Technol. **8**, 897 (1994).

5. S. P. Timoshenko and J. N. Goodier, Theory of Elasticity, McGraw-Hill, New York (1970), Chapt. 12.

6. J. E. Houston, G. E. Franklin and T. A. Michalske (In preparation).

7. See, for example: R. W. Hertzberg, Deformation and Fracture Mechanics of Engineering Materials, John Wiley and Sons, New York 1989, Chap. 2.

8. G. M. Pharr, T. Y. Tsui, A. Boshakov and W. C. Oliver, Mat. Res. Soc. Proc. **338**, 127 (1994).

9. Flexus, Inc., Sunnyvale, CA.

10. Digital Instruments Inc, 520 E. Montecito St. Santa Barbara, CA 93103.

11. K. F. Jarausch, J. E. Houston and P. E. Russell (In Preparation).

12. R. Q. Hwang, J. D. Kiely and J. E. Houston (In Preparation).

13. A program modification of the "Shoescan" STM softwary by B. S. Swartzentruber of Sandia National Laboratories.

14. See, for example: O. L. Alerhand, D. Vanderbilt, R. D. Meade and J. D. Joannopoulos, Phys. Rev. Lett. **61**, 1973 (1988); B. S. Swartzentruber, N. Kitamura, M. G. Lagally and M. B. Webb, Phys. Rev. B **47**, 13432 (1993).